JACS
JOURNAL OF THE AMERICAN CHEMICAL SOCIETY

pubs.acs.org/JACS

Article

Computational Design and Synthesis of a Deeply Red-Shifted and Bistable Azobenzene

David B. Konrad,*,▽ Gökcen Savasci,▽ Lars Allmendinger, Dirk Trauner, Christian Ochsenfeld,* and Ahmed M. Ali*

Cite This: J. Am. Chem. Soc. 2020, 142, 6538−6547

Read Online

ACCESS | Metrics & More | Article Recommendations | Supporting Information

ABSTRACT: We computationally dissected the electronic and geometrical influences of *ortho*-chlorinated azobenzenes on their photophysical properties. X-ray analysis provided the insight that *trans*-tetra-*ortho*-chloro azobenzene is conformationally flexible and thus subject to molecular motions. This allows the photoswitch to adopt a range of red-shifted geometries, which account for the extended n → π* band tails. On the basis of our results, we designed the di-*ortho*-fluoro di-*ortho*-chloro (**dfdc**) azobenzene and provided computational evidence for the superiority of this substitution pattern to tetra-*ortho*-chloro azobenzene. Thereafter, we synthesized **dfdc** azobenzene by *ortho*-chlorination via 2-fold C−H activation and experimentally confirmed its structural and photophysical properties through UV−vis, NMR, and X-ray analyses. The advantages include near-bistable isomers and an increased separation of the n → π* bands between the *trans*- and *cis*-conformations, which allows for the generation of unusually high levels of the *cis*-isomer by irradiation with green/yellow light as well as red light within the biooptical window.

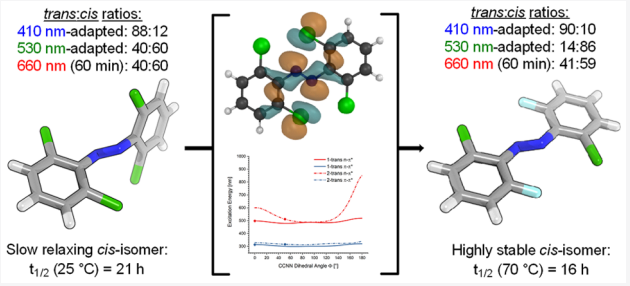

INTRODUCTION

Azobenzenes are versatile photoswitches that can be cycled between their *cis*- and *trans*-configurations with light.[1,2] Because of their small size, robust photoswitching, synthetic accessibility, and low rate of photobleaching, they serve as excellent building blocks for the generation of elaborate optical tools.[3−5] Photopharmaceuticals, for example, contain azobenzene fragments as ON- and OFF-switches, which allow for the control of biological functions with the spatiotemporal precision of light.[6−11] To elicit the full potential of these optical tools and to apply them to complex animal tissues, it is crucial to use tissue-penetrating, nonhazardous red and near-infrared (NIR) light within the biooptical window[12] (650−950 nm).[13−15] In addition, it is highly desirable to use photoswitches with slow thermal relaxation rates for the less stable isomers and near-quantitative photoconversion for each isomer. Fast-relaxing photopharmaceuticals require constant illumination with high intensity light for their photoswitching to outcompete the thermal relaxation. This becomes increasingly difficult in deeper tissue layers.[16] The bathochromic shift, the thermal stability, and the photoconversion strongly depend on the substitution pattern of the azobenzene core.[7,16,17] Therefore, the design of new photopharmaceuticals that are operated at the biooptical window relies on the availability of azobenzene photoswitches with the appropriate photophysical properties.

A strategy for generating red-shifted photoswitches entails the separation of the n → π* absorption bands, which are typically overlapping for *cis*- and *trans*-azobenzene in the visible spectrum. In this context, a significant advancement was made through tetra-*ortho*-substitution with heteroatoms.[18−21] Tetra-*ortho*-methoxy azobenzenes, for instance, have long-lived *cis*-isomers ($\tau \approx 2$ d) and are readily photoswitched to their *trans*- and *cis*-configurations with blue and green/red light, respectively.[20] Modification of the tetra-*ortho*-methoxy pattern with electron-donating substituents implements an azonium ion, which can be isomerized with near-infrared light (up to 720 nm) but suffers from a significant decrease in the thermal stability of the *cis*-isomer ($\tau = 1$ s).[22,23] In contrast, the *cis*-isomer of the tetra-*ortho*-fluoro azobenzene has a thermal half-life on the order of years ($t_{1/2} = 700$ d) and can be reliably photoswitched with blue (*trans*-configuration) and green (*cis*-configuration) light.[19,20] Significant photoconversion to the *cis*-isomer can be reached with up to 527 nm light.[24] The use of longer wavelengths requires the use of an alternative substitution pattern such as the tetra-*ortho*-chloro azoben-

Received: September 27, 2019
Published: March 24, 2020

https://dx.doi.org/10.1021/jacs.9b10430
J. Am. Chem. Soc. 2020, 142, 6538−6547

zene.[24] It is worth noting that certain photoswitches can be operated with light in the near-infrared region (NIR) by using two-photon excitation.[25] Because of the slow photoswitching through two-photon excitation, however, this approach requires the use of photoswitches with long-lived isomers to reach significant photoconversion.[26]

Remarkably, tetra-*ortho*-chloro azobenzenes allow for rapid and efficient photoswitching by irradiation of the n → π* band tails. For example, the fastest isomerization rate to the photostationary state (PSS) with the highest content of the *cis*-isomer for alkyl-substituted derivatives, such as *red*-**AzCA-4** (Figure 1), was reached by using green light (550−560 nm),

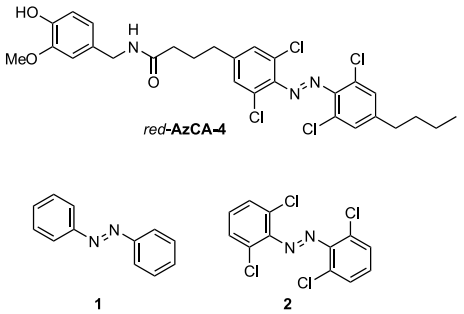

Figure 1. Structures of *red*-**AzCA-4**, azobenzene (**1**), and tetra-*ortho*-chloro azobenzene (**2**).

although the λ_{max} of the *trans*-isomer (400 nm-adapted) lies close to 450 nm.[27] It was further demonstrated that irradiation at far ends of the n → π* band can still produce a PSS with a significant *cis*-content by using bright light sources and continuous irradiation. For instance, Woolley and co-workers[28] reported photoswitching of tetra-*ortho*-chloro azobenzenes with high intensity red light (625 nm) for 1 min, whereas Feringa and co-workers[24] applied longer-wavelength high intensity red light (652 nm) for 2.5 h to reach a PSS with the highest levels of the *cis*-isomer.

Intrigued by the potential of the tetra-*ortho*-chloro substitution pattern (Figure 1) as a basis to develop new photoswitches with long-lived *cis*-isomers, near-quantitative PSS, and excitation wavelengths within the biooptical window, we focus our study on the evaluation of the influence of azobenzene *ortho*-chlorination on the photophysical properties. By dissecting the effects of the chlorination into its geometric and electronic subcomponents, we aim to identify the origin of the extended red-shifted n → π* band tails of *ortho*-chlorinated azobenzenes as well as the separation of the n → π* excitation between the *trans*- and *cis*-isomers. Therefore, we employed a combination of quantum-chemical methodologies as well as X-ray analyses. On the basis of our results, the tetra-*ortho* substitution pattern could be optimized to yield a photoswitch with a highly stable *cis*-isomer and PSS with high contents for each isomer while retaining the red-shifted transition.[29,30]

We first computed the geometries of our studied azobenzene substitution patterns as well as their π → π* and n → π* absorption bands. Previous studies have shown that employing a PBE0 hybrid functional provides the closest correlation between the computational and experimental results for determining the λ_{max} of azobenzene-based photoswitches.[31] Therefore, we optimized the structures for all studied photoswitches on the PBE0-D3/def2-TZVP[32−35] level of theory using the TURBOMOLE program package, to obtain the respective gas-phase ground-state minimum geometry at 0 K followed by the computation of the vertical excitation energies on the TD-PBE0/def2-TZVP level. This gives access to absorption maxima (λ_{max}) of the π → π* (S0 → S2) as well as the n → π* (S0 → S1) transitions for optimized *trans*- and *cis*-azobenzene geometries.

EFFECTS OF THE AZOBENZENE *ORTHO*-CHLORINATION

The geometrical changes in the conformation of azobenzenes through isomerization or substitution can be subdivided into three main categories: changes in the N−N bond length, the C(1)−C(2)−N(3)−N(4) dihedral angles Φ, and the C(2)−N(3)−N(4)−C(5) dihedral angle Ψ (Figure 2). The CCNN

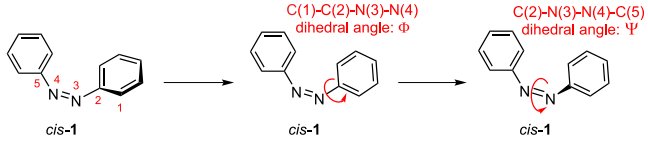

Figure 2. Numerical descriptors for the dihedral angles.

dihedral angles describe the rotation of the aryl rings out of the plane. This rotation can proceed from two directions and thus can be described by two dihedral angles for each aryl ring: Φ_S and Φ_L. We focus our discussion on the smaller Φ_S angles. The Ψ dihedral angle describes the distortion of the N−N double bond.

For the evaluation of the influence of tetra-*ortho*-chlorination on the bathochromic shifts of azobenzene, we computationally optimized structures for *trans*-**1**, *cis*-**1**, *trans*-**2**, and *cis*-**2** and verified that their conformations are true minima on the potential energy surface (PES). We found that *trans*-azobenzene has a planar structure with an N−N bond length of 1.242 Å and N−N bond geometry (Ψ dihedral angle) of 180.0°. The structure of *trans*-tetra-*ortho*-chloro azobenzene is characterized by the rotation of both aryl rings out of the plane by 50.8° (Φ_S). In addition, the N−N bond length is shortened to 1.236 Å, and the N−N double bond is slightly distorted to 175.3° (Ψ). Next, we determined their n → π* (S0 → S1) absorption bands (Table 1) and found that the conversion of

Table 1. Optimized Conformations of 1 and 2: Vertical Excitation Energies (TD-PBE0/def2-TZVP) and Photoswitch Structures (PBE0-D3/def2-TZVP)

comp.	N=N [Å]	Φ_S [deg]	Ψ [deg]	S0 → S1 [nm]
trans-**1**	1.242	0.0	180.0	483.6
cis-**1**	1.234	52.0	8.5	470.0
trans-**2**	1.236	50.8	175.3	498.5
cis-**2**	1.229	60.5	5.1	474.9

azobenzene (**1**) to **2** induces a bathochromic shift of the n → π* absorption band of 14.9 and 4.9 nm for the *trans*- and *cis*-isomers, respectively. Because of the higher red-shift for the *trans*-isomer, the overall difference between the excitation band maxima of both configurations increases from 13.6 nm (**1**) to 23.6 nm (**2**). This increased band separation allows for the generation of PSS with higher contents of *cis*-isomers by irradiation of the *trans*-**2** n → π* excitation band as compared to that of *trans*-**1**.

To get a more detailed understanding of the effects of the *ortho*-chloro substituents, we studied mono-, di-, tri-, and tetra-chlorinated azobenzenes (Figure 3 and Table 2). Substituting

https://dx.doi.org/10.1021/jacs.9b10430
J. Am. Chem. Soc. 2020, 142, 6538−6547

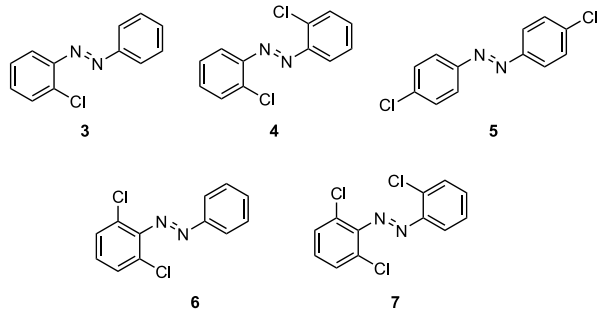

Figure 3. Mono-, di-, and trichlorinated azobenzenes.

Table 2. Mono-, Di-, Tri-, and Tetrachlorinated Azobenzenes: Vertical Excitation Energies (TD-PBE0/def2-TZVP) and Photoswitch Structures (PBE0-D3/def2-TZVP)

	config.	N=N [Å]	$\Phi_S(Ar^1)$ [deg]	$\Phi_S(Ar^2)$ [deg]	Ψ [deg]	S0 → S1 [nm]
1	*trans*	1.242	0.0	0.0	180.0	483.6
	cis	1.234	52.0	52.0	8.5	470.0
3	*trans*	1.242	0.2	1.4	179.9	501.9
	cis	1.232	51.7	63.0	9.5	454.3
4	*trans*	1.243	0.7	2.7	179.8	520.6
	cis	1.231	63.0	63.0	10.5	438.6
5	*trans*	1.243	0.1	0.1	180.0	480.0
	cis	1.235	50.5	50.5	9.0	478.7
6	*trans*	1.239	0.6	53.6	178.1	483.6
	cis	1.230	50.4	74.3	6.9	444.5
7	*trans*	1.239	10.6	49.8	179.1	502.8
	cis	1.230	51.7	71.8	7.8	453.9
2	*trans*	1.236	50.8	50.8	175.3	498.5
	cis	1.229	60.5	60.5	5.1	474.9

one *ortho*-hydrogen on **1** for chlorine (**3**) already leads to a significant separation of the n → π* transition band of the *trans*- and *cis*-isomers. As compared to **1**, *trans*-**3** is red-shifted by 18.3 nm, and *cis*-**3** is blue-shifted by 15.7 nm. Because both structures *trans*-**1** and *trans*-**3** remain planar, the bathochromic shift could be attributed to the electronic contribution of the chlorination. The chlorinated aryl ring of *cis*-**3** has an increased Φ_S angle by 11.0°. Because of the asymmetric structure, both aryl rings are rotated at different Φ angles. In this case, the average of both smaller Φ_S angles, Φ_S(avg), can be used as a descriptor for the overall rotation. For example, changing the substitution pattern from *cis*-**1** to *cis*-**3** results in a difference of 5.4° in the Φ_S(avg) (52.0 nm for *cis*-**1** and 57.4 nm for *cis*-**3**). Appending a second *ortho*-chlorine at the opposite aryl ring follows the same trend and provides absorption maxima at 520.6 nm (*trans*-**4**) and 438.6 nm (*cis*-**4**). To evaluate the origin of the strong shifts in the n → π* excitation wavelengths through *ortho*-chloro substitution, we investigated the photophysical properties of *para*-chloro azobenzene (**5**). If the bathochromic shift is a result of the extended π-system and the concomitant effects on the π* molecular orbital (MO), *para*-chloro azobenzene **5** should behave in a fashion similar to that of the *ortho*-substituted derivative **4**. The n → π* vertical excitation energies of di-*para*-chloro azobenzene (**5**), however, are comparable to those of azobenzene (**1**). Therefore, the excitation wavelength shifts are an effect of the substitution at the *ortho*-position. Because the *ortho*-chlorine atoms of *trans*-**4** are facing toward the nitrogen lone pairs, it is reasonable to assume that their repulsive interaction destabilizes the n molecular orbital and thus decreases the energy gap to the π* molecular orbital.[18] In contrast, the bent structure of *cis*-**4** allows the chlorine atoms to face in the opposite directions of the nitrogen lone pairs. We reason that the strong blue-shift of the n → π* excitation band that is observed by transitioning from *cis*-**1** to *cis*-**4** results from a withdrawal of electron density through the electronegative chlorine substituents in proximity to the N−N bond. This effect has previously been reported for tetra-*ortho*-fluoro azobenzenes and leads to a lowering of the n-orbital energy.[19,36]

In contrast to **4**, the introduction of the second *ortho*-chlorine on the same aryl ring (**6**) twists the chlorinated aryl group of the *trans*-isomer out of the plane at a Φ_S angle of 53.6° and leads to a hypsochromic shift of the n → π* excitation energy. On the basis of our prior findings, we hypothesize that the hypsochromic shift is a result of a decreased interaction between the chlorine substituent and the nitrogen lone pairs due to the rotation of the aryl ring. Changing the substitution pattern from *cis*-**4** to *cis*-**6** only results in minor changes in the Φ_S(avg) angle (63.0 nm for *cis*-**4** and 62.4 nm for *cis*-**6**), which is reflected by the subtle n → π* band shift from 438.6 to 444.5 nm. It is worth noting that the rotation around the Φ dihedral angle for *trans*-**6** is accompanied by a contraction of the N−N bond length from 1.243 to 1.239 Å, which is retained in the more chlorinated derivatives **7**. Adding a third *ortho*-chlorine onto **6** induces a red-shift of the n → π* excitation energy of the *trans*-**7** and *cis*-**7** of 19.2 and 9.4 nm, respectively. Finalizing the transition to tetra-*ortho*-chloro azobenzene (**2**) from **7** strongly increases the rotational overall twist of the *trans* structure to 50.8° for both Φ_S angles. This distortion leads to a further contraction of the N−N bond length from 1.239 Å (*trans*-**7**) to 1.236 Å (*trans*-**2**). In addition, a strong contraction of the Ψ dihedral angle to 175.3° occurs, which ranges between 178.1° and 180.0° in the *trans*-configuration of less chlorinated substrates (**1**, **3**−**7**). The structural and conformational changes were accompanied by an n → π* hypsochromic shift of 4.3 nm. In contrast to *trans*-**2**, *cis*-**2** is subject to a strong n → π* bathochromic shift of 21 nm. We reasoned that the increasing substitution of the *ortho*-position decreases the rotational flexibility of the individual aryl rings around the Φ dihedral angle. As a consequence, the chlorine atoms of *cis*-**2** are forced into the proximity of the nitrogen lone pairs, which destabilizes

Table 3. Optimized Conformation of 2 Imposed on the Structure of 1 (A,B) and Conformation of 1 Imposed on 2 (C,D): Vertical Excitation Energies (TD-PBE0/def2-TZVP) and Photoswitch Structures (PBE0-D3/def2-TZVP)

entry	comp.	N=N [Å]	Φ_S [deg]	Ψ [deg]	S0 → S1 [nm]
A	*trans*-**1** (*trans*-**2**-adopted)	1.236	50.8	175.3	443.7
B	*cis*-**1** (*cis*-**2**-adopted)	1.229	60.5	5.1	471.4
C	*trans*-**2** (*trans*-**1**-adopted)	1.242	0.0	180.0	711.3
D	*cis*-**2** (*cis*-**1**-adopted)	1.234	52.0	8.5	463.1

https://dx.doi.org/10.1021/jacs.9b10430
J. Am. Chem. Soc. 2020, 142, 6538−6547

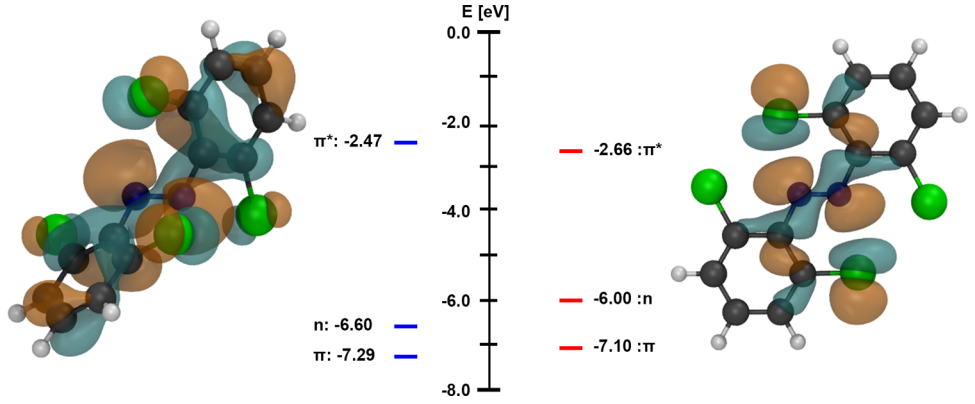

Figure 4. Computed orbital energies and n-MO densities of the optimized **2** conformation (left) and the conformation of **1** imposed on **2** (right).

the n molecular orbital and decreases the energy gap between the n → π^* transition.

EXAMINING THE EFFECT OF THE TETRA-*ORTHO*-CHLORO AZOBENZENE CONFORMATION ON ITS EXCITATION ENERGY

The computational study of the stepwise *ortho*-chlorination of azobenzene (**1**) to tetra-*ortho*-chloro azobenzene (**2**) highlights that the geometry of the respective photoswitch has a strong influence on the n → π^* excitation energies. To determine whether the conformational changes of the same photoswitch structures provide shifts in the excitation energies, we calculated the vertical excitation energies of **1** adopting the optimized conformations of **2** (Table 3, entries A and B) as well as the vertical excitation energies of **2** adopting the optimized conformations of **1** (entries C and D). Because the conformations of *cis*-**1** and *cis*-**2** are closely related, imposing the *cis*-**2** geometry onto *cis*-**1** and vice versa did not provoke any significant alterations of its photophysical properties. In contrast, changing the 3D structure of azobenzene to the tilted geometry of **2** leads to a blue-shift of 39.9 nm for n → π^* transitions. Imposing the planar *trans*-**1** geometry onto *trans*-**2** leads to an outstanding n → π^* bathochromic shift of 212.8 nm. This result supports the theoretical hypothesis that the photophysical properties of an azobenzene-based photoswitch are determined by both the chemical composition and the conformational geometry.[20] It furthermore showcases the profound effect a change in the conformation can have on the n → π^* excitation wavelength of tetra-*ortho*-chloro azobenzenes. By computing the MO energies and visualizing the MOs of the optimized and the planar *trans*-**2** conformations (Figure 4), we show that the strong n → π^* bathochromic shift likely originates from the increased interaction between the chlorine and the nitrogen lone pair, which leads to a strong destabilization of the n-MO by 0.60 eV (Figure 4 and Table 3). The planar geometry additionally stabilizes the π^*-MO, which decreases the gap of the n → π^* transition.

To gain a more detailed understanding of the influence of the azobenzene conformation, we evaluated each of the main geometrical variables for **1** and **2** separately (Figure 5 and Supporting Information, Chapter 2.8 and Figure S74). Therefore, we simulated the contraction and elongation of the N−N bond lengths (Figure S74A and B), the distortion of the Ψ dihedral angles (Figure S74C), and the selective rotation of one aryl ring around the Φ dihedral angles (Figures 5 and S74E). In each case, elongating the optimized N−N bond

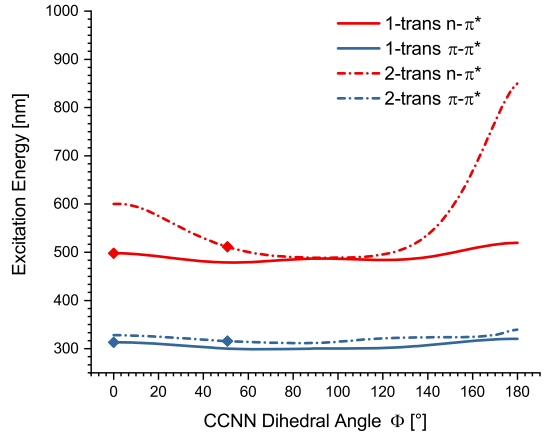

Figure 5. Influence of the C−C−N−N dihedral angle Φ_S on the excitation energy: optimized structure (PBE0-D3/def2-TZVP) with the corresponding vertical excitation energies (TD-PBE0/def2-SVP) of the photoswitches **1** and **2**.

lengths (Figure S74A and B) results in a bathochromic shift of the n → π^* excitation bands with the strongest shifts for *trans*-tetra-*ortho*-chloro azobenzene (**2**). A distortion of the Ψ dihedral angles (Figure S74C) by contracting the *trans*-**1** and *trans*-**2** structures as well as bending the *cis*-**1** and *cis*-**2** structures evokes a bathochromic shift. Rotating one aryl ring of *trans*-**1** around the Φ dihedral angle (Figure 5) has minor effects on the n → π^* transition. The *trans*-**2** n → π^* excitation energies, however, were subject to a strong red-shift when the Φ angle approached 0° and 180° (Figure 5). In case of *cis*-**1**, rotating one aryl ring (Figure S74E) around the CCNN axis shows that approaching planarity with the N−N double bond in either direction provides a red-shift of n → π^* excitation energies. We found that the steric bulk of the *ortho*-chlorine atoms hinders the full rotation around the CCNN axis of *cis*-**2** (Figure S74E and F). Slight rotations of the optimized *cis*-**2** geometry have minor effects on the n → π^* excitation energy, whereas approaching the limit of the rotational axis in each direction strongly decreases the excitation energy barrier.

In general, our quantum-chemical calculations have shown that the n → π^* vertical excitation energy of *trans*-**2** is strongly dependent on its conformation and that minor structural changes, such as the elongation of the N−N bond length, distortion of the Ψ dihedral angle, and rotations of the Φ dihedral angles can lead to strong bathochromic shifts. To compare our computational findings to experimental conformations of azobenzene (**1**) and tetra-*ortho*-chloro azoben-

https://dx.doi.org/10.1021/jacs.9b10430
J. Am. Chem. Soc. 2020, 142, 6538−6547

zene (**2**), we recrystallized *trans*-**2** as well as *cis*-**2** and analyzed their structures using X-ray crystallography.

X-RAY ANALYSIS OF TETRA-*ORTHO*-CHLORO AZOBENZENE

To gain insight into the experimental 3D structures of tetra-*ortho*-chloro azobenzenes, we investigated *trans*-**2** and *cis*-**2** using X-ray crystallography (Figure 6 and Table 4). In

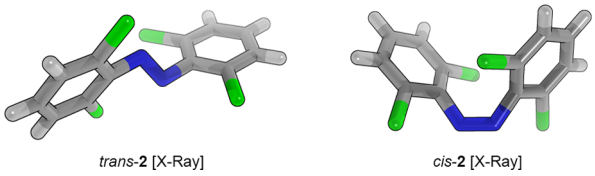

Figure 6. X-ray structures of *trans*-**2** and *cis*-**2**.

Table 4. X-ray Analysis of the Structural Flexibility

	config.	N=N [Å]	$\Phi_S(Ar^1)$ [deg]	$\Phi_S(Ar^2)$ [deg]	Ψ [deg]
1	*trans*	1.249	9.7	9.7	180.0
	cis	1.251	51.6	51.6	7.7
2	*trans*^{1}	1.182	35.2	79.7	180.0
	trans^2	1.245	51.6	65.4	178.1
	trans^3	1.248	53.1	59.3	176.3
	cis	1.251	57.0	63.6	3.5

accordance with our computational results, we found that the steric bulk of the *ortho*-chlorine atoms twists the two aryl rings of *trans*-**2** out of the plane. Remarkably, the extended cell of the crystal structure contains three conformations for *trans*-**2** with strong variations between the conformations. For example, the N−N bond length ranges from 1.182 to 1.248 Å, the Φ_S dihedral angles reach from 35.2° to 79.7°, and the Ψ dihedral angle is distorted from 180.0° to 176.3°. This result is an essential cornerstone for the development of new photoswitches, because it provides a new perspective on tetra-*ortho*-substituted azobenzenes: the twisted *trans*-isomers are not stiff structures but are highly flexible and subject to molecular motions. In contrast, the *trans*-azobenzene (**1**) X-ray structure contains one conformation, which is near-planar with a N−N bond length of 1.249, an ideal nondistorted Ψ angle, and a Φ_S dihedral of 9.7°.[37] The X-ray structures *cis*-**1**[38] and *cis*-**2** also contain a single conformation, which suggests that these structures have a more restricted conformation as compared to that of *trans*-**2**. Conformational NMR studies by Brittain and co-workers,[39] however, have shown that *cis*-tetra-*ortho*-substituted azobenzenes are subject to a certain degree of structural flexibility. Comparing the structures of the *cis*-isomers shows that the relative changes in the conformation are accurately portrayed by our quantum-chemical calculations. For instance, the average distortion of the Φ_S dihedral angle is increased from 51.6° (*cis*-**1**) to 60.3° (*cis*-**2**), and the Ψ dihedral angle is decreased from 7.7° (*cis*-**1**) to 3.5° (*trans*-**2**).

We hypothesize that the broad n → π* excitation bands and the concomitant extended band tail that allow for the photoswitching to PSS with a high *cis*-content with red light are a result of the conformational flexibility of *trans*-**2**. We have provided computational evidence that azobenzene-based photoswitches are subject to strong changes in their excitation energies through the slightest alterations in their conformation. Consequentially, we deduce that the excitation of the n → π* bands at the red end of the spectrum is affected by highly red-shifted conformations. The low absorption intensity of the tail regions is a result of the low abundance of the conformations that are shifted into the red region. According to our calculations, highly red-shifted conformations are characterized by long N−N bonds, small Φ_S angles, and/or distorted Ψ angles. In contrast, the strong absorption intensity of the band maxima is a result of the high abundance of conformations that are closely related to the optimized structures. Irradiation at the band tail thus allows for the photoswitching of red-shifted conformations to the *cis*-isomer. On the basis of our hypothesis, *trans*-**2** continuously cycles through a variety of 3D structures, which include these red-shifted conformations. Therefore, a PSS with a high *cis*-content can be reached with red light by the gradual accumulation of the long-lived *cis*-isomer, while the flexible *trans*-**2** molecules continuously adopt red-shifted conformations and are photoswitched.

It is reasonable to assume that a large fraction of the highly red-shifted conformations is characterized by small average Φ_S angles, due to the outstanding n → π* band shifts that result from the interaction between the chlorine atoms and the nitrogen lone pairs. Therefore, we envisage that modifying the substitution pattern to allow for a more planar structure yields a photoswitch that could be isomerized using red light within the biooptical window. Substituting one *ortho*-chlorine atom on each aryl ring of **2** for the smaller fluorine atoms, in this context, may lead to smaller Φ_S dihedral angles and thereby enable a better overlap between the two retained chlorine atoms and the nitrogen lone pairs. In addition, incorporation of fluorine atoms leads to a stronger withdrawal of electron density in proximity to the diazene unit. This effect is known to produce a hypsochromic shift of the n → π* band of the *cis*-isomer, which increases the separation of the excitation energies between both isomers.[19,36] Irradiation of the individual bands close to the absorption maxima could consequently result in a PSS with higher isomer levels using shorter light pulses.

COMPUTATIONAL OPTIMIZATION OF THE TETRA-*ORTHO* SUBSTITUTION PATTERN

A computational investigation of the substitution of two *ortho*-chlorines of **2** for the more electronegative fluorine (**8**, Figure 7) shows that, in accordance with our hypothesis, the Φ_S dihedral angles decrease from 50.8° to 37.3°. In addition, the N−N bond is lengthened from 1.236 to 1.243 Å, and the distortion of the Ψ angle is nearly retained. The combination of these structural changes induces a bathochromic shift of 9.1 nm by transitioning from *trans*-**2** to *trans*-**8** (Table 5).

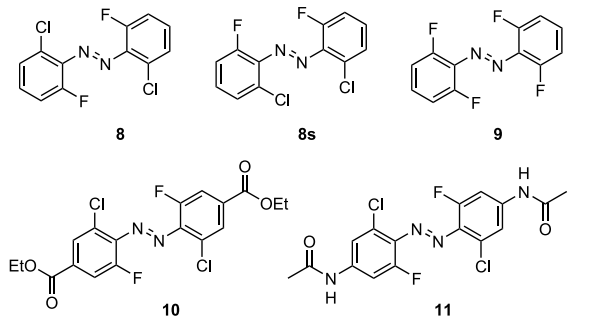

Figure 7. Structures of di-*ortho*-fluoro di-*ortho*-chloro (**dfdc**, **8**), tetra-*ortho*-fluoro (**9**) azobenzene, as well as the **dfdc** derivatives **10** and **11**.

https://dx.doi.org/10.1021/jacs.9b10430
J. Am. Chem. Soc. 2020, 142, 6538−6547

Table 5. Exchange of Two Chlorine Atoms for Fluorine on Tetra-*ortho*-chloro Azobenzene: Vertical Excitation Energies (TD-PBE0/def2-TZVP) and Photoswitch Structures (PBE0-D3/def2-TZVP)

	config.	N=N [Å]	$\Phi_S(Ar^1)$ [deg]	$\Phi_S(Ar^2)$ [deg]	Ψ [deg]	S0 → S1 [nm]
2	*trans*	1.236	50.8	50.8	175.3	498.5
	cis	1.229	60.5	60.5	5.1	474.9
8	*trans*	1.243	37.3	37.3	175.7	507.6
	cis	1.232	58.6	58.6	8.4	452.7
8s	*trans*	1.241	37.6	42.8	175.5	508.0
	cis	1.231	56.4	66.8	6.8	452.4
9	*trans*	1.246	27.7	27.7	176.7	505.5
	cis	1.233	59.5	59.5	8.9	440.5
10	*trans*	1.242	40.5	40.5	175.1	526.9
	cis	1.233	60.9	60.9	6.6	450.6
11	*trans*	1.248	27.0	27.0	176.7	523.2
	cis	1.234	57.1	57.1	9.8	463.8

Comparing *cis*-**2** to *cis*-**8** showed a stronger distortion of the Ψ angle and an increased N−N bond length from 1.229 to 1.232 Å, without any significant alteration of the Φ_S dihedral angle. Although these geometric adjustments have been shown to contribute to a bathochromic shift, the electronic contribution to the photophysical properties that stem from the withdrawing effect of the fluorine atoms results in an overall hypsochromic shift of 22.2 nm. To exclude the possibility that the di-*ortho*-fluoro di-*ortho*-chloro (**dfdc**) azobenzene preferentially adopts a conformation, where the chlorines are arranged on the same face of the molecule (**8s**), we computed the total energies of both structures. The optimized geometries *trans*-**8** and *cis*-**8** are more stable by 4.0 kJ/mol than are *trans*-**8s** and *cis*-**8s**, respectively (Table 5). To evaluate the differences between the newly designed tetra-*ortho*-fluoro/tetra-*ortho*-chloro hybrid (**8**) and the literature-known tetra-*ortho*-fluoro structure (**9**),[19,36] we investigated **9** with the same quantum-chemical methodology. As expected, transitioning from *cis*-**8** to *cis*-**9** does not significantly alter the conformation, but the increased withdrawal of electron density in proximity to the diazene unit leads to a hypsochromic shift of 12.2 nm. In comparison to *trans*-**8**, *trans*-**9** is approaching a planar conformation. The Φ_S angle decreased to 27.7°, the Ψ angle increased to 176.7°, and the N−N double bond is elongated to 1.246 Å. These combined structural changes lead to a positioning of the n → π* excitation maxima (*trans*-**9**: λ_{max} = 505.5 nm) similar to that of *trans*-**8**. On the basis of our previous findings, however, we hypothesize that the geometric flexibility of *trans*-**8** enables an overlap between the bulky chlorine atoms with the nitrogen lone pairs through molecular motions. This interaction strongly contributes to the extended n → π* band tails and allows for photoswitching with red light. The small fluorine atoms of *trans*-**9**, in comparison, are unable to overlap with the n molecular orbitals to the same extent, which leads to narrower n → π* absorption bands and photoswitching with wavelengths close to the λ_{max}.

To account for the influence of electronically active substituents on the conformation and photophysical properties of the **dfdc** azobenzene, we computationally investigated the addition of ethyl benzoate (**10**) and acetamide (**11**) groups to its *para*-positions. Transitioning from *trans*-**8** to *trans*-**10** and from *cis*-**8** to *cis*-**10** does not show any significant geometrical changes, respectively. The electron-withdrawing effect of the ethyl benzoate substituents (**10**), however, leads to a strong bathochromic shift of 19.3 nm for *trans*-**10** and a slight hypsochromic shift of 2.1 nm of *cis*-**10**. Implementing an electron-rich substitution pattern (**11**) on the **dfdc** azobenzene backbone leads to an elongation of the N−N bond from 1.243 Å (*trans*-**8**) to 1.248 Å for *trans*-**11**, which is accompanied by a relaxation of the twisted geometry by decreasing the Φ_S dihedral angle from 37.3° to 27.0°, whereas no significant alterations are observed for the *cis*-**11** conformation. For the combination of these structural properties with the electron-donating effect of the acetamide substituents, we observe a bathochromic shift of 15.6 nm for *trans*-**11** and of 11.1 nm for *cis*-**11**.

SYNTHESIS AND PHOTOPHYSICAL CHARACTERIZATION OF DI-*ORTHO*-FLUORO DI-*ORTHO*-CHLORO AZOBENZENE

To confirm our theoretical results and to evaluate whether the designed hybrid combines the red-shift of the tetra-*ortho*-chloro azobenzene *trans*-isomer with the blue-shift of the tetra-*ortho*-fluoro azobenzene *cis*-isomer, we synthesized **8**. In addition, we were intrigued by the strong computed bathochromic shift that occurred by substituting *trans*-**8** with two ethyl benzoate substituents (*trans*-**10**) and synthesized **10** to experimentally validate the effect of an electron-withdrawing *para*-substituent on the photophysical properties of **dfdc** azobenzenes. For these syntheses, we leveraged our previously established C−H chlorination methodology.[27] By optimizing this methodology for the dichlorination of the di-*ortho*-fluoro azobenzenes **12** and **13**, we could increase its substrate scope to mixed *ortho*-substituted azobenzenes and provide our desired products **8** and **10** in ample quantities (Figure 8).

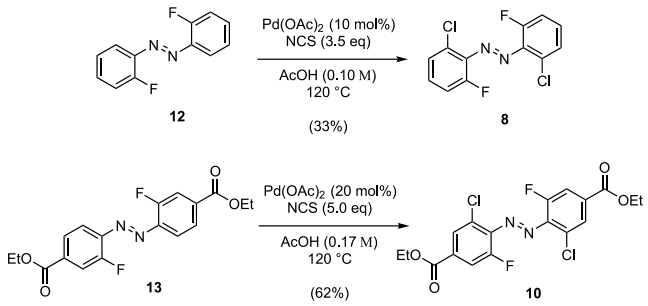

Figure 8. Synthesis of the tetra-*ortho*-hydrids **8** and **10** using a palladium-catalyzed C−H chlorination.

In general, the positions of the π → π* and n → π* excitation bands were determined through UV−vis analysis using a 50 μM solution in DMSO. Because of the low absorption of the n → π* transition, the visualization of the full extent of the band tail required a measurement at higher concentrations (500 μM solution in DMSO).[40] After the position of the excitation bands was determined, the extent of the n → π* band tail was verified through photoswitching by illuminating the compounds with light at the red end of the visible spectrum (Figure 9). The light-dependent PSS were then analyzed by NMR spectroscopy using a 500 μM solution in DMSO-d6 to allow for a direct comparison with the UV−vis spectra. For example, the n → π* of *trans*-azobenzene (*trans*-**1**) absorbs light up to 550 nm (Figure 9c). This was experimentally confirmed by irradiation of the dark-adapted state with green/yellow light (see the Supporting Information).

https://dx.doi.org/10.1021/jacs.9b10430
J. Am. Chem. Soc. 2020, 142, 6538−6547

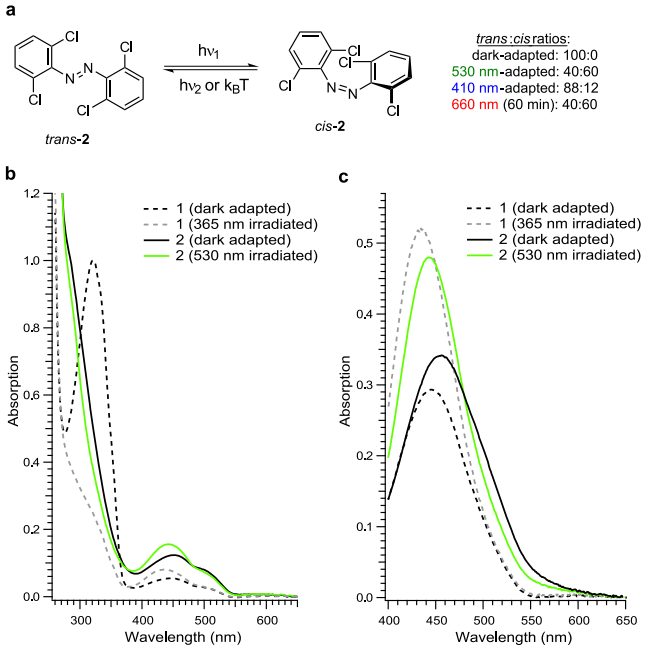

Figure 9. (a) Photoswitching of tetra-*ortho*-chloro azobenzene (**2**). UV−vis spectra of **1** and **2**: (b) 50 μM in DMSO is used to show the full spectrum and (c) 500 μM in DMSO is used to visualize the extent of the n → π^* band tails.

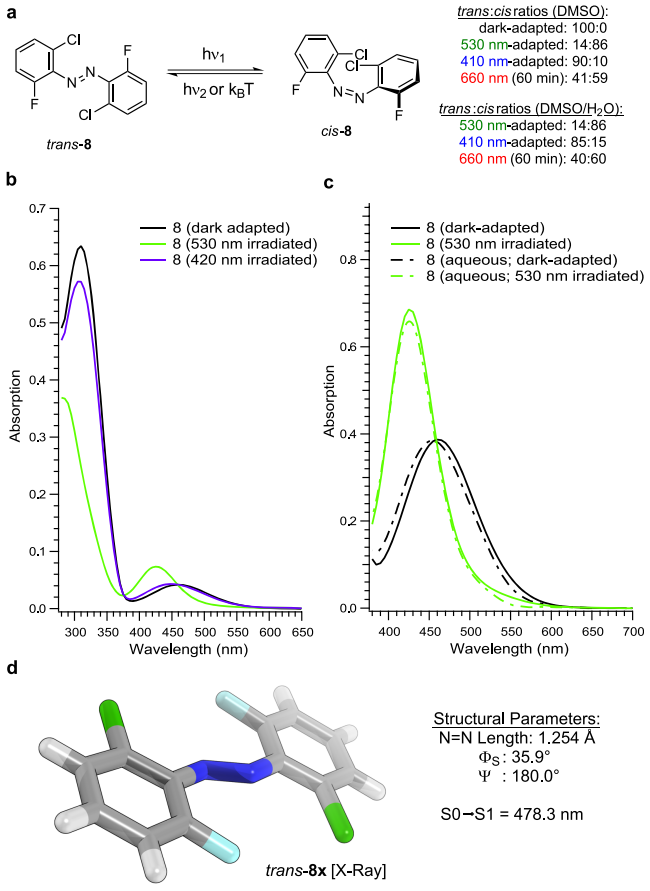

Figure 10. (a) Photoswitching of di-*ortho*-fluoro di-*ortho*-chloro azobenzene (**8**). UV−vis spectra of **8**: (b) 50 μM in DMSO is used to show the full spectrum; (c) 500 μM in DMSO and 9:1 DMSO:H_2O are used to visualize the extent of the n → π^* band tails; and (d) X-ray structure of *trans*-**8x** and its calculated vertical excitation energy (TD-PBE0/def2-TZVP).

Illumination with 590 nm does not effect a change in the UV−vis spectrum, whereas 530 nm light produces an altered PSS of the molecule (**1**). However, due to the substantial overlap of the n → π^* excitation bands of the *trans*- and *cis*-isomers, the application of 530 nm light only leads to minor photoconversion in comparison to irradiation of the π → π^* band maximum with UV-A light. UV−vis analysis of tetra-*ortho*-chloro azobenzene (**2**, Figure 9) shows slightly separated n → π^* band tails with a more red-shifted absorption spectrum for the dark-adapted state (100% *trans*-isomer). This slight separation of the n → π^* band tails allows one to reach significant photoconversion by irradiating with green light (530 nm, *trans*:*cis* = 40:60). The extent of the tail was determined by applying 660 nm red light with an intensity of 24.1 mW/cm^2 to the blue-adapted (410 nm) compound, which produces a *trans*:*cis* ratio of 40:60 after 60 min. Both azobenzene (**1**) and tetra-*ortho*-chloro azobenzene (**2**) have long-lived *cis*-isomers with thermal half-lives of 75.5 and 20.7 h in DMSO at 25 °C, respectively.

Remarkably, by exchanging two chlorine atoms of **2** for fluorine (**8**), the separation between the n → π^* excitation bands of the *trans*-isomer and *cis*-isomer of **8** strongly improved, which allows for the generation of near-quantitative PSS (Figure 10). Irradiation with green light (530 nm), for example, leads to an excellent PSS with significantly increased *cis*-isomer content (*trans*:*cis* = 14:86) as compared to **2** (530 nm, *trans*:*cis* = 40:60). In addition, high levels of *trans*-**8** (*trans*:*cis* = 90:10) could be produced with blue light (410 nm). The extent of the n → π^* band tail was determined by applying 660 nm light (24.1 mW/cm^2) to the blue-adapted compound, which produces a *trans*:*cis* ratio of 41:59 after 60 min, 20:80 after 120 min, and even reaches 3:97 after 300 min. By employing a deeply red LED with higher intensity (660 nm, 32.3 mW/cm^2) under the same setting, photoswitching could be accelerated to provide *trans*:*cis* ratios of 30:70 and 10:90 after 60 and 120 min, respectively. To further increase the rate of photoswitching, a three-membered LED array could be used (660 nm; 24.1, 32.3, and 44.3 mW/cm^2), which leads to a *trans*:*cis* ratio of 24:76 after 60 min, 13:87 after 90 min, and 5:95 after 120 min. Next, we investigated the thermal half-lives of **8** and found that it is near-bistable. Full relaxation of green-irradiated **8** (530 nm) to its *trans*-configuration requires heating to 90 °C for 7 h ($t_{1/2}$ = 2 h, DMSO). The thermal half-life at 70 °C was determined to be 16 h in DMSO. X-ray analysis of *trans*-**8** provides the conformation *trans*-**8x** where both aryl rings are oriented on parallel, slightly displaced planes. In comparison to *trans*-**2**, *trans*-**8x** has a decreased Φ_S angle (Φ_S = 35.9°), a diminished distortion of the Ψ angle (Ψ = 180°), and an elongated N−N bond length (N−N = 1.254 Å), which is in accordance with our calculations. By subjecting *trans*-**8x** to our quantum-chemical methodology, we determined that the n → π^* absorption maximum of the X-ray conformation lies at 478.3 nm, which is a hypsochromic shift of 29.3 nm as compared to *trans*-**8**. On the basis of this result, it is likely that the highly red-shifted conformations are adopted in the process of transitioning between the twisted *trans*-**8** and *trans*-**8x**, where both aryl rings are oriented on parallel, slightly displaced planes.

https://dx.doi.org/10.1021/jacs.9b10430
J. Am. Chem. Soc. 2020, 142, 6538−6547

We assessed the utility of the **dfdc** azobenzene as a photoswitch for the development of photopharmaceuticals by analyzing its photophysical properties in an aqueous solution (9:1 DMSO:H_2O). Overall, we did not observe any significant changes in the PSS and thermal stability by transitioning from DMSO to a mixture of DMSO and water. The PSS that is reached with green light (530 nm, *trans*:*cis* = 14:86) remains unchanged, and irradiation with blue light (410 nm, *trans*:*cis* = 85:15) only decreases the content of the *trans*-isomer by a small fraction. Prolonged irradiation (60 min) of the blue-adapted photoswitch (410 nm) with deep red light (660 nm, 24.1 mW/cm^2, *trans*:*cis* = 40:60) produces a PSS similar to that from irradiation in DMSO. The thermal half-life of *cis*-**8** at 70 °C is 12 h in 9:1 DMSO:H_2O.

To confirm that the **dfdc** azobenzene (**8**) is subject to a stronger bathochromic shift than are both of its parent azobenzenes, we examined the extent of the n → π^* excitation band of tetra-*ortho*-fluoro azobenzene (**9**). UV−vis analysis shows that the n → π^* band tail of **9** does not exceed 590 nm (see the Supporting Information for experimental details), which was subsequently confirmed by NMR analysis. Irradiating the blue-adapted tetra-*ortho*-fluoro azobenzene (420 nm, *trans*:*cis* = 83:17) with yellow light (595 nm, 10.1 mW/cm^2) for 60 min provided a slight change in the PSS (*trans*:*cis* = 76:14). However, subjecting **9** to a 60 min pulse of red light (625 nm, 26.7 mW/cm^2) or deep red light (660 nm, 24.1 mW/cm^2) did not provide a significant alteration of the *trans*:*cis* ratio.

Next, we examined the effect of electron-withdrawing *para*-substituents on the photophysical properties of the **dfdc** azobenzene by implementing ethyl benzoate groups (**10**, Figure 11). As compared to *trans*-**8** and *cis*-**8**, the λ_{max}(n → π^*) values of both isomers, *trans*-**10** and *cis*-**10**, are subject to a bathochromic shift (Figure 11c). This provides an excellent separation of the n → π^* excitation bands between the *trans*- and *cis*-isomers in the blue as well as orange/red regions of the visible spectrum and a stronger overlap in the green region. Therefore, green light (530 nm) produces a *trans*:*cis* ratio of 41:59, whereas photoswitching with 410 and 440 nm blue light results in outstanding PSS with *trans*-isomer contents of 96% and 95%, respectively. This effect is further demonstrated by irradiating the 410 nm-adapted **10** with deep red light (660 nm, 24.1 mW/cm^2), which shows accelerated photoswitching kinetics as compared to **8** and produces a *trans*:*cis* ratio of 17:83 after 60 min. The only drawback of the electron-poor **10** as compared to the unsubstituted **dfdc** azobenzene is the diminished thermal stability of the *cis*-isomer, which has a half-life of 5 h at 25 °C in DMSO.

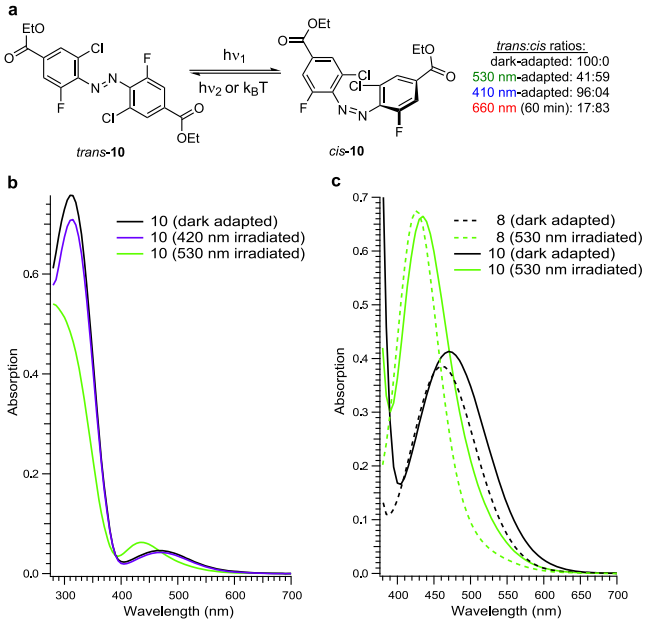

Figure 11. (a) Photoswitching of the electron-poor di-*ortho*-fluoro di-*ortho*-chloro azobenzene **10**. UV−vis spectra of **8** and **10**: (b) 50 μM in DMSO is used to show the full spectrum; and (c) 500 μM in DMSO is used to visualize the extent of the n → π^* band tails.

SIGNIFICANCE OF THE DI-*ORTHO*-FLUORO DI-*ORTHO*-CHLORO AZOBENZENE

Azobenzenes are the most commonly used photoswitches to develop advanced optical tools such as photopharmaceuticals, due to their small size, robust photoswitching, and low rate of photobleaching.[1−5] To fine-tune the photophysical properties of these optical devices, it is highly desirable to have access to an arsenal of azobenzene core structures with defined photophysical properties. In this regard, the **dfdc** azobenzene (**8**) provides an unprecedented solution to the long-standing problem to identify a substitution pattern that combines near-bistable isomers, PSS with high levels of *trans*- and *cis*-isomers, and photoswitching within the biooptical window. Although photoswitching with deep red light (660 nm) requires long irradiation times (*trans*:*cis* = 41:59 after 60 min with 24.1 mW/cm^2), we show that by increasing the light intensity (*trans*:*cis* = 30:70 after 60 min with 32.3 mW/cm^2) and/or using arrays of multiple LEDs (*trans*:*cis* = 24:76 after 60 min with 24.1, 32.3, and 44.3 mW/cm^2), the photoswitching rate can be significantly accelerated. In addition, the installation of electron-poor substituents on the **8** *para*-position (**10**) is accompanied by a bathochromic shift, which allows for faster isomerization with deep red light. Given that photodynamic therapy is carried out with light sources that provide an intensity of up to 200 mW/cm^2 which can, in theory, be incorporated into an array, we reason that the **dfdc** azobenzene could be photoswitched within a photopharmaceutically relevant time frame in a therapeutic setting.[41] The decreased steric bulk of the *ortho*-substitution of **8** as compared to **2** allows the relaxation of the twisted structure to a near-planar geometry, which leads to a closer 3D relationship of **dfdc** azobenzene to azobenzene. This factor plays a crucial role in the process of red-shifting photopharmaceuticals.[42] The ability to add a *para*-substituent to **8** increases the utility of this pattern by allowing its anchoring to optical devices through an electron-active substituent (**10**). This substitution pattern leads to a shift of the λ_{max}(n → π^*) to the red end of the spectrum, increases the *trans*-content of the blue-irradiated photoswitch, and only decreases the thermal stability of the *cis*-isomer to an extent that **10** is still considered a slow-relaxing azobenzene. These excellent photophysical properties that were demonstrated by evaluating two **dfdc** derivatives leave a great margin for improvement with regard to the substitution of the *meta*- and *para*-positions. Therefore, **8** serves an ideal basis for the development of a photoswitch that operates with near-infrared light while retaining highly bistable isomers by performing an in-depth investigation into the effects of alternative substitution patterns on its photophysical properties.

https://dx.doi.org/10.1021/jacs.9b10430
J. Am. Chem. Soc. 2020, 142, 6538−6547

CONCLUSION AND OUTLOOK

We have used a combination of quantum-chemical calculations and X-ray analyses to dissect the effects of the *ortho*-chlorination in its electronic and structural subcomponents and identified the origin of the extended red-shifted n → π^* band tails of tetra-*ortho*-chloro azobenzenes. On the basis of our findings, we designed the **dfdc** azobenzene substitution pattern and synthesized **8** and **10** by employing a C−H dichlorination methodology. UV−vis and NMR studies showed significant improvements of the photophysical properties of **8** over the tetra-*ortho*-chloro and tetra-*ortho*-fluoro substitution pattern. Photoswitching can be achieved with red light within the biooptical window and provides a PSS with up to 97% of the highly stable *cis*-isomer. These outstanding properties make the **dfdc** azobenzene an ideal photoswitch for the development of photopharmaceuticals that target complex animal tissues. In addition, the **dfdc** azobenzene scaffold is an excellent basis for the development of bistable photoswitches that can be isomerized with near-infrared light. Implementing an electron-poor substitution pattern by adding an ethyl benzoate group to both *para*-positions (**10**), for example, leads to a significant bathochromic shift of the n → π^* excitation bands of both isomers, which results in an accelerated photoconversion by applying deep red light as compared to **8**. To evaluate the full potential of the **dfdc** azobenzene, studies on the effect of *meta*- and *para*-substituents are currently underway.

ASSOCIATED CONTENT

Supporting Information

The Supporting Information is available free of charge at https://pubs.acs.org/doi/10.1021/jacs.9b10430.

Experimental procedures, spectroscopic data, and copies of NMR spectra (PDF)

X-ray crystallographic data for compounds *trans*-**2** (CCDC 1954066), *cis*-**2** (CCDC 1954067), and *trans*-**8x** (CCDC 1954065) (CIF)

AUTHOR INFORMATION

Corresponding Authors

Ahmed M. Ali − *Department of Pharmacy and Department of Chemistry, Ludwig-Maximilians-University Munich, Munich 81377, Germany; Department of Medicinal Chemistry, Faculty of Pharmacy, Assiut University, Assiut 71515, Egypt*; Email: ahmed.ali@cup.uni-muenchen.de

Christian Ochsenfeld − *Department of Chemistry, Ludwig-Maximilians-University Munich, Munich 81377, Germany; Max Planck Institute for Solid State Research, Stuttgart 70569, Germany*; orcid.org/0000-0002-4189-6558; Email: c.ochsenfeld@fkf.mpg.de

David B. Konrad − *Department of Pharmacy and Department of Chemistry, Ludwig-Maximilians-University Munich, Munich 81377, Germany; Department of Chemistry, The Scripps Research Institute, La Jolla, California 92037, United States*; orcid.org/0000-0001-5718-8081; Email: david.konrad@cup.lmu.de

Authors

Gökcen Savasci − *Department of Chemistry, Ludwig-Maximilians-University Munich, Munich 81377, Germany; Max Planck Institute for Solid State Research, Stuttgart 70569, Germany*; orcid.org/0000-0002-6183-7715

Lars Allmendinger − *Department of Pharmacy, Ludwig-Maximilians-University Munich, Munich 81377, Germany*

Dirk Trauner − *Department of Chemistry, Ludwig-Maximilians-University Munich, Munich 81377, Germany; Department of Chemistry, New York University, New York, New York 10003, United States*; orcid.org/0000-0002-6782-6056

Complete contact information is available at: https://pubs.acs.org/10.1021/jacs.9b10430

Author Contributions

[▽]D.B.K. and G.S. contributed equally.

Notes

The authors declare no competing financial interest.

ACKNOWLEDGMENTS

This work was supported by the SFB749 to D.T. and C.O. as well as a Georg Forster Research Fellowship (Alexander von Humboldt Foundation) to A.M.A. C.O. also acknowledges financial support by the Innovative Training Network "Computational Spectroscopy in Natural Sciences and Engineering" (ITN-COSINE). D.B.K. received funding from the European Union's Framework Program for Research and Innovation Horizon 2020 (2014-2020) under the Marie Skłodowska-Curie Grant agreement no. 754388 (LMUResearchFellows) and from LMU Munich's Institutional Strategy LMUexcellent within the framework of the German Excellence Initiative (no. ZUK22). A.M.A. is grateful to Prof. Dr. Klaus Wanner for hosting the second year of his AvH fellowship. We thank Prof. Ivan Huc for hosting revision experiments in his laboratory, Dr. Oliver Thorn-Seshold and Li Gao for their help with establishing a LED setup, Dr. Peter Mayer for X-ray analyses, as well as Marvin Thielert for helpful discussions.

REFERENCES

(1) Bandara, H. M. D.; Burdette, S. C. Photoisomerization in different classes of azobenzene. *Chem. Soc. Rev.* **2012**, *41*, 1809−1825.

(2) Hartley, G. S. The Cis-form of Azobenzene. *Nature* **1937**, *140*, 281.

(3) Merino, E. Synthesis of azobenzenes: the coloured pieces of molecular materials. *Chem. Soc. Rev.* **2011**, *40*, 3835−3853.

(4) Clara, B.; Falk, R.; Alexander, G.; Günter, M.; Alexander, H. Light-Controlled Tools. *Angew. Chem., Int. Ed.* **2012**, *51*, 8446−8476.

(5) Dong, L.; Feng, Y.; Wang, L.; Feng, W. Azobenzene-based solar thermal fuels: design, properties, and applications. *Chem. Soc. Rev.* **2018**, *47*, 7339−7368.

(6) Timm, F.; Schönberger, M.; Dirk, T. Optochemical Genetics. *Angew. Chem., Int. Ed.* **2011**, *50*, 12156−12182.

(7) Beharry, A. A.; Woolley, G. A. Azobenzene photoswitches for biomolecules. *Chem. Soc. Rev.* **2011**, *40*, 4422−4437.

(8) Broichhagen, J.; Frank, J. A.; Trauner, D. A Roadmap to Success in Photopharmacology. *Acc. Chem. Res.* **2015**, *48*, 1947−1960.

(9) Lerch, M. M.; Hansen, M. J.; van Dam, G. M.; Szymanski, W.; Feringa, B. L. Emerging Targets in Photopharmacology. *Angew. Chem., Int. Ed.* **2016**, *55*, 10978−10999.

(10) Szymański, W.; Beierle, J. M.; Kistemaker, H. A. V.; Velema, W. A.; Feringa, B. L. Reversible Photocontrol of Biological Systems by the Incorporation of Molecular Photoswitches. *Chem. Rev.* **2013**, *113*, 6114−6178.

(11) Velema, W. A.; Szymanski, W.; Feringa, B. L. Photopharmacology: Beyond Proof of Principle. *J. Am. Chem. Soc.* **2014**, *136*, 2178−2191.

(12) Hammerich, M.; Schütt, C.; Stähler, C.; Lentes, P.; Röhricht, F.; Höppner, R.; Herges, R. Heterodiazocines: Synthesis and Photochromic Properties, Trans to Cis Switching within the Biooptical Window. *J. Am. Chem. Soc.* **2016**, *138*, 13111−13114.

(13) Frangioni, J. V. In vivo near-infrared fluorescence imaging. *Curr. Opin. Chem. Biol.* **2003**, *7*, 626−634.
(14) Smith, A. M.; Mancini, M. C.; Nie, S. Second window for in vivo imaging. *Nat. Nanotechnol.* **2009**, *4*, 710.
(15) Weissleder, R. A clearer vision for in vivo imaging. *Nat. Biotechnol.* **2001**, *19*, 316.
(16) Dong, M.; Babalhavaeji, A.; Samanta, S.; Beharry, A. A.; Woolley, G. A. Red-Shifting Azobenzene Photoswitches for in Vivo Use. *Acc. Chem. Res.* **2015**, *48*, 2662−2670.
(17) Bléger, D.; Hecht, S. Visible-Light-Activated Molecular Switches. *Angew. Chem., Int. Ed.* **2015**, *54*, 11338−11349.
(18) Beharry, A. A.; Sadovski, O.; Woolley, G. A. Azobenzene Photoswitching without Ultraviolet Light. *J. Am. Chem. Soc.* **2011**, *133*, 19684−19687.
(19) Knie, C.; Utecht, M.; Zhao, F.; Kulla, H.; Kovalenko, S.; Brouwer, A. M.; Saalfrank, P.; Hecht, S.; Bléger, D. ortho-Fluoroazobenzenes: Visible Light Switches with Very Long-Lived Z Isomers. *Chem. - Eur. J.* **2014**, *20*, 16492−16501.
(20) Samanta, S.; Beharry, A. A.; Sadovski, O.; McCormick, T. M.; Babalhavaeji, A.; Tropepe, V.; Woolley, G. A. Photoswitching Azo Compounds in Vivo with Red Light. *J. Am. Chem. Soc.* **2013**, *135*, 9777−9784.
(21) Samanta, S.; McCormick, T. M.; Schmidt, S. K.; Seferos, D. S.; Woolley, G. A. Robust visible light photoswitching with ortho-thiol substituted azobenzenes. *Chem. Commun.* **2013**, *49*, 10314−10316.
(22) Dong, M.; Babalhavaeji, A.; Collins, C. V.; Jarrah, K.; Sadovski, O.; Dai, Q.; Woolley, G. A. Near-Infrared Photoswitching of Azobenzenes under Physiological Conditions. *J. Am. Chem. Soc.* **2017**, *139*, 13483−13486.
(23) Dong, M.; Babalhavaeji, A.; Hansen, M. J.; Kalman, L.; Woolley, G. A. Red, far-red, and near infrared photoswitches based on azonium ions. *Chem. Commun.* **2015**, *51*, 12981−12984.
(24) Wegener, M.; Hansen, M. J.; Driessen, A. J. M.; Szymanski, W.; Feringa, B. L. Photocontrol of Antibacterial Activity: Shifting from UV to Red Light Activation. *J. Am. Chem. Soc.* **2017**, *139*, 17979−17986.
(25) Kellner, S.; Berlin, S. Two-Photon Excitation of Azobenzene Photoswitches for Synthetic Optogenetics. *Appl. Sci.* **2020**, *10*, 805.
(26) Cabré, G.; Garrido-Charles, A.; Moreno, M.; Bosch, M.; Porta-De-La-Riva, M.; Krieg, M.; Gascón-Moya, M.; Camarero, N.; Gelabert, R.; Lluch, J. M.; Busqué, F.; Hernando, J.; Gorostiza, P.; Alibés, R. Rationally designed azobenzene photoswitches for efficient two-photon neuronal excitation. *Nat. Commun.* **2019**, *10*, 907.
(27) Konrad, D. B.; Frank, J. A.; Trauner, D. Synthesis of Redshifted Azobenzene Photoswitches by Late-Stage Functionalization. *Chem. - Eur. J.* **2016**, *22*, 4364−4368.
(28) Rullo, A.; Reiner, A.; Reiter, A.; Trauner, D.; Isacoff, E. Y.; Woolley, G. A. Long wavelength optical control of glutamate receptor ion channels using a tetra-ortho-substituted azobenzene derivative. *Chem. Commun.* **2014**, *50*, 14613−14615.
(29) Calbo, J.; Weston, C. E.; White, A. J. P.; Rzepa, H. S.; Contreras-Garcéa, J.; Fuchter, M. J. Tuning Azoheteroarene Photoswitch Performance through Heteroaryl Design. *J. Am. Chem. Soc.* **2017**, *139*, 1261−1274.
(30) Weston, C. E.; Richardson, R. D.; Haycock, P. R.; White, A. J. P.; Fuchter, M. J. Arylazopyrazoles: Azoheteroarene Photoswitches Offering Quantitative Isomerization and Long Thermal Half-Lives. *J. Am. Chem. Soc.* **2014**, *136*, 11878−11881.
(31) Simeth, N. A.; Bellisario, A.; Crespi, S.; Fagnoni, M.; König, B. Substituent Effects on 3-Arylazoindole Photoswitches. *J. Org. Chem.* **2019**, *84*, 6565−6575.
(32) Ahlrichs, R.; Bär, M.; Häser, M.; Horn, H.; Kölmel, C. Electronic structure calculations on workstation computers: The program system turbomole. *Chem. Phys. Lett.* **1989**, *162*, 165−169.
(33) Grimme, S.; Antony, J.; Ehrlich, S.; Krieg, H. A consistent and accurate ab initio parametrization of density functional dispersion correction (DFT-D) for the 94 elements H-Pu. *J. Chem. Phys.* **2010**, *132*, 154104.
(34) Weigend, F. Accurate Coulomb-fitting basis sets for H to Rn. *Phys. Chem. Chem. Phys.* **2006**, *8*, 1057−1065.
(35) Weigend, F.; Häser, M.; Patzelt, H.; Ahlrichs, R. RI-MP2: optimized auxiliary basis sets and demonstration of efficiency. *Chem. Phys. Lett.* **1998**, *294*, 143−152.
(36) Bléger, D.; Schwarz, J.; Brouwer, A. M.; Hecht, S. o-Fluoroazobenzenes as Readily Synthesized Photoswitches Offering Nearly Quantitative Two-Way Isomerization with Visible Light. *J. Am. Chem. Soc.* **2012**, *134*, 20597−20600.
(37) Harada, J.; Ogawa, K. X-ray Diffraction Analysis of Non-equilibrium States in Crystals: Observation of an Unstable Conformer in Flash-Cooled Crystals. *J. Am. Chem. Soc.* **2004**, *126*, 3539−3544.
(38) Mostad, A.; Rømming, C. A. Refinement of the Crystal Structure of cis-Azobenzene. *Acta Chem. Scand.* **1971**, *25*, 3561−3568.
(39) Rastogi, S. K.; Rogers, R. A.; Shi, J.; Gao, C.; Rinaldi, P. L.; Brittain, W. J. Conformational Dynamics of o-Fluoro-Substituted Z-Azobenzene. *J. Org. Chem.* **2015**, *80*, 11485−11490.
(40) Wang, D.; Wagner, M.; Butt, H.-J.; Wu, S. Supramolecular hydrogels constructed by red-light-responsive host-guest interactions for photo-controlled protein release in deep tissue. *Soft Matter* **2015**, *11*, 7656−7662.
(41) Bäumler, W. Light sources for photodynamic therapy and fluorescence diagnosis in dermatology. In *Comprehensive Series in Photosciences*; Calzavara-Pinton, P., Szeimies, R.-M., Ortel, B., Eds.; Elsevier: New York, 2001; Vol. 2, Chapter 6, pp 83−98.
(42) Trads, J. B.; Burgstaller, J.; Laprell, L.; Konrad, D. B.; de la Osa de la Rosa, L.; Weaver, C. D.; Baier, H.; Trauner, D.; Barber, D. M. Optical control of GIRK channels using visible light. *Org. Biomol. Chem.* **2017**, *15*, 76−81.

https://dx.doi.org/10.1021/jacs.9b10430
J. Am. Chem. Soc. 2020, 142, 6538−6547